

December 12, 2001

Dark Matter Detection Rates In SUGRA Models

R. ARNOWITT AND B. DUTTA

*Center For Theoretical Physics, Department of Physics,
Texas A&M University, College Station TX 77843-4242*

Direct detection of Milky Way wimps are discussed within the framework of R-parity conserving SUGRA models with grand unification at M_G . Two questions are discussed: what SUGRA models can account for the DAMA data if this data is confirmed, and is the full SUGRA parameter space accessible to future planned detectors. Experimental constraints of the Higgs mass bound, the $b \rightarrow s\gamma$ bound, relic density constraints (including all co-annihilation channels), etc. are imposed. In addition, the effect of the possible muon $g - 2$ anomaly are examined. For mSUGRA, we find that the Higgs mass and $b \rightarrow s\gamma$ constraint puts a lower bound $m_{1/2} > (300 - 400)$ GeV (i.e. $m_{\tilde{\chi}_1^0} > (120 - 160)$ GeV) for $\tan\beta < 50$, and thus the largest theoretical neutralino-proton cross sections still lie significantly below the DAMA 3σ lower bound. (Predictions for $\tan\beta > 50$ become sensitive to the precise value of m_t and m_b .) If in addition one imposes the muon anomaly constraint, μ must be positive and an upper bound of $m_{1/2} < 850$ GeV for $\tan\beta < 50$ is obtained. More generally, if $\mu > 0$ and $m_{1/2} < 1$ TeV, the cross sections are $\gtrsim 10^{-10}$ pb, and hence this parameter space would be mostly accessible to planned high sensitivity detectors. For non-minimal SUGRA models, the cross sections can be considerably larger, and a simple SU(5) model with non-universal soft breaking in the Higgs and third generation is seen to give cross sections in the DAMA range for $\tan\beta \gtrsim 15$ with $m_{\tilde{\chi}_1^0} > 80$ GeV, and minimum cross sections $\gtrsim 10^{-10}$ pb for $\mu > 0$.

PRESENTED AT

COSMO-01

Rovaniemi, Finland,
August 29 – September 4, 2001

1 Introduction

It is generally agreed that a large part of the Milky Way galaxy is made of dark matter, i.e. current estimates of the dark matter energy density are $\rho_{\text{DM}} \simeq (0.3 - 0.5)\text{GeV}/\text{cm}^3$. However, what this dark matter is made of is much less clear, and many suggestions exist. We will here assume a SUSY explanation, and in particular assume that the dark matter particle is the lightest supersymmetric particle (the LSP), the lightest neutralino, $\tilde{\chi}_1^0$. A number of ways have been suggested to detect SUSY wimps: One may look for annihilation in the halo of the Galaxy leading to $\tilde{\chi}_1^0 + \tilde{\chi}_1^0 \rightarrow e^+, \bar{p} + X$ and search for the anti-particle signals. Alternately, one expects neutralinos to be captured by the Sun or Earth, fall into their center and there annihilate. Muon neutrinos could then escape, and one could look for the signal $\tilde{\chi}_1^0 + \tilde{\chi}_1^0 \rightarrow \nu_\mu + X$ with neutrino telescopes on Earth. Finally, there is the possibility of direct detection by the scattering of incident neutralinos by terrestrial nuclear targets.

The theoretical expectations for these possible signals depends upon the model chosen. The most general SUSY model, the MSSM, contains over 100 free parameters (63 real parameters!), and so it does not have great predictive power. The supergravity (SUGRA) models with grand unification at the GUT scale $M_G \simeq 2 \times 10^{16} \text{ GeV}$ [1, 2], apply to a wide range of phenomena, and are relatively predictive. We will consider here then the SUGRA models, both those with universal soft breaking (mSUGRA) and non-universal soft breaking at the GUT scale. Our models will also possess R-parity invariance, to guarantee the existence of a stable LSP dark matter candidate. In particular we examine the gravity mediated models. (Other possibilities such as gauge mediated soft breaking have difficulty in constructing a viable dark matter candidate, while the anomaly mediated models appear to be in contradiction with the recent Brookhaven muon magnetic moment data.)

Concerning possible signals, there has been indications of an excess of \bar{p} and e^+ events in the halo, indicating possible halo $\tilde{\chi}_1^0$ annihilations. This data is quite interesting and has led to some recent analyses [3, 4], though it is difficult to be sure of all the astrophysical backgrounds. Analyses have also been given of the possibilities for present or future neutrino telescopes (AMANDA, Ice Cube, ANTARES) to see energetic ν_μ from the Sun [5, 6]. Thus [5] finds that Ice Cube and ANTARES can be sensitive to $\tilde{\chi}_1^0$ -annihilation for non-universal SUGRA models but only for large $\tan\beta$ i.e. $\tan\beta \gtrsim 35$. The most promising way of detecting halo wimps for a wide range of parameters remains, then, direct detection by terrestrial targets, and we will restrict the discussion to this possibility from now on.

Experiments for direct detection of Milky Way wimps is now entering a new (and exciting) phase. There exists the DAMA results with data that indicates the observation of the annual modulation signal (at the $4\text{-}\sigma$ level), and the CDMS exclusion curves which appear to exclude much of the allowed DAMA region. However, there are a number of new experiments that should be able to clarify matters in the relatively near future. Thus DAMA is constructing an upgrade to a 250 kg NaI detector (from their current 95 kg

detector). Two other detectors that will be completed in the near future, GENIUS-TF and ZEPLIN II, should be able to give independent observations of whether the annual modulation effect exists, and when CDMS is moved to the SOUDAN mine, its exclusion curves will be sensitive to the full DAMA allowed region. Further, in the more distant future, a number of new detectors are being planned with much higher sensitivity, e.g. GENIUS, Cryoarray, ZEPLIN IV, and CUORE.

In view of this, we consider here two questions: (1) If the DAMA data is confirmed, what SUGRA models can account for the relatively large neutralino-proton cross sections this data implies, and (2) what are the lowest SUGRA cross sections theoretically predicted, and will the planned detectors be able to scan the full SUGRA parameter space. We will see that the DAMA data, if confirmed, would exclude the mSUGRA model (but be consistent with non-universal models), and if the Brookhaven $g_\mu - 2$ anomaly is valid, future detectors will be able to test SUGRA models over the full parameter space and hence be competitive with accelerator experiments.

2 Experimental and Theoretical Constraints

One of the important features of SUGRA models is that they apply to a wide range of phenomena, and data from these already restrict the parameter space and thus strengthen the predictions. We list here the main experimental constraints that we use.

(1) Higgs mass

The LEP data [7] places the lower bound of $m_h > 114$ GeV. However, theoretical calculation of the light Higgs mass, m_h , still have an uncertainty of about 3 GeV. Thus we will conservatively interpret the experimental bound to require that the theoretically calculated mass obey $m_h > 111$ GeV.

(2) $b \rightarrow s\gamma$ branching ratio

The CLEO data [8] has both systematic and theoretical uncertainties. We therefore take a relative broad range around the CLEO central value of

$$1.8 \times 10^{-4} \leq B(B \rightarrow X_s \gamma) \leq 4.5 \times 10^{-4} \quad (1)$$

(3) $\tilde{\chi}_1^0$ relic density

The cosmic microwave background radiation (CMB) and other data now give a relatively constrained value for the cosmic mass density of dark matter. This is measured in terms of the value of $\Omega_{\text{DM}} h^2$. Here $\Omega_{\text{DM}} = \rho/\rho_c$ where ρ is mass density of dark matter, and $\rho_c = 3H^2/8\pi G_N$ is the critical density to close the universe ($H = (100 \text{ km/sMpc})h$ is the current Hubble constant, G_N is the Newton constant). A recent analysis gives $\Omega_{\text{DM}} h^2 = 0.139 \pm 0.026$ [9]. We take a 2.5σ range around the mean:

$$0.07 \leq \Omega_{\text{DM}} h^2 \leq 0.021 \quad (2)$$

In looking for the minimum cross section, we conservatively extend this range to be from 0.025 to 0.25.

(4) Recently, the BNL E821 experiment [10] has observed a 2.6σ anomaly in the muon magnetic moment $a_\mu = (g_\mu - 2)/2$. Such an anomaly was predicted some time ago for mSUGRA models [11, 12] and we will thus interpret the affect as being due to SUGRA. We take here a 2σ range around the E821 central value

$$11 \times 10^{-10} \leq a_\mu^{\text{SUGRA}} \leq 75 \times 10^{-10} \quad (3)$$

While this effect is not yet certain (and there is some debate as to the size of the Standard Model hadronic contribution, see e.g.[13]), it has a significant impact on dark matter prediction. We will therefore include it in our analysis, but show explicitly what effects it produces. Further data, currently being analyzed by E821, should reduce both the experimental error and theoretical uncertainty by more than a factor of two, and results should be available early next year *.

In order to carry out accurate calculations, it is necessary to include a number of theoretical corrections, and we list some of these here. (1) Two loop gauge and one loop Yukawa renormalization group equations (RGE) are used from M_G to the electroweak scale M_{EW} and QCD RGE are used below for the light quark contributions. We chose $M_{\text{EW}} = (m_{\tilde{t}_L} m_{\tilde{t}_R})^{1/2}$. (2) Two loop and pole mass corrections are included in the calculation of m_h . (3) One loop corrections to m_b and m_τ [14, 15] are included which are important for large $\tan\beta$. (4) Large $\tan\beta$ NLO SUSY corrections to $b \rightarrow s\gamma$ [16, 17] are included. (5) All stau-neutralino co-annihilation channels are included in the relic density calculation, this analysis being done for both small and large $\tan\beta$ [18, 19, 20]. We note that we do not include Yukawa unification or proton decay constraints, as these depend sensitively on post-GUT physics about which little is known. (For example, string theory with e. g. an SU(5) GUT group requires grand unification of the gauge coupling constants, just as SUGRA theory does, but the Yukawa or proton decay constraints of SUGRA need not apply [21].)

3 mSUGRA Model

The minimal supergravity model, mSUGRA, is the most predictive of the models as it depends on only four additional parameters and one sign. It is convenient to chose these parameters as follows: m_0 , the scalar soft breaking mass at M_G ; $m_{1/2}$, the gaugino soft breaking mass as M_G . (We note here the approximate formulae that $m_{\tilde{\chi}_1^0} \simeq 0.4m_{1/2}$,

*Recently, two papers have appeared (Knecht et.al. (hep-ph/0111059), Hayakawa and Kinoshita (hep-ph/0112102)) implying a sign error in the scattering of light by light contribution to a_μ . This reduces the 2.6σ effect to 1.6σ , our lower bound then becomes 1σ below the central value. We note that with the further data, the E821 experiment would be expected to see an $\simeq 4\sigma$ effect, if the reduced central value were to remain unchanged

the chargino mass $m_{\tilde{\chi}_1^\pm} \simeq 0.8m_{1/2}$, and the gluino mass $m_{\tilde{g}} \simeq 2.5m_{1/2}$); A_0 , the cubic soft breaking mass at M_G ; $\tan\beta = \langle H_2 \rangle / \langle H_1 \rangle$ at the electroweak scale (where $H_{(2,1)}$ gives rise to up,down quark masses); and the sign of μ , the Higgs mixing parameter (which appears in the superpotential as $\mu H_1 H_2$). We examine these parameters over the following range: $m_0, m_{1/2} \leq 1$ TeV, $2 \leq \tan\beta \leq 50$, and $A_0 \leq 4m_{1/2}$. The range of m_0 and $m_{1/2}$ is sufficient to explore the full range that will be accessible to the LHC (and we will see that if the $g_\mu - 2$ anomaly is real, it will cover the full parameter space). There is a small additional allowed region of very high $\tan\beta$ i. e. $\tan\beta \simeq 50 - 55$. However, as we will see below that predictions in this region are very sensitive to the precise values of the t and b quark masses which are not at present known.

In general, the neutralino-nucleus scattering cross section has a spin dependent part and a spin independent part. However, the transition from quark to proton scattering for heavy nuclei, the spin independent cross section dominates, and this allows one to extract (to a good approximation) $\sigma_{\tilde{\chi}_1^0-p}$, the neutralino-proton cross section, from any dark matter detector data. The basic quark diagrams for neutralino-quark scattering, $\sigma_{\tilde{\chi}_1^0-q}$, are s-channel scattering through first generation squarks, and t-channel scattering through h and H (where H is the heavy neutral Higgs boson). One can determine $\sigma_{\tilde{\chi}_1^0-p}$ then from the basic quark scattering. However, this can involve errors perhaps of a factor of $\lesssim 2$ from uncertainties in the strange quark content of the proton and the pion-nucleon σ term, $\sigma_{\pi-N}$. (We use here the most recent evaluations of the σ term, $\sigma_{\pi-N} = 65$ MeV [22, 23]. Earlier evaluations, $\sigma_{\pi-N} \simeq 45$ MeV, would reduce the cross sections by perhaps a factor of 2.)

The parameter space for calculations of the above detector cross section are constrained significantly by the requirement that the theory predict the right amount of relic neutralino dark matter. In the early universe, two neutralinos can annihilate to Standard Model particles through s-channel Z , h , H and A poles (A is the CP odd Higgs boson), and through t-channel sfermion diagrams. However, if a second particle becomes nearly degenerate with the $\tilde{\chi}_1^0$, one must include it in the early universe annihilation processes, leading to the phenomena of co-annihilation. In SUGRA models with universal gaugino masses at the GUT scale, this “accidental” near degeneracy occurs naturally for the light stau, $\tilde{\tau}_1$. To see this semi-quantitatively, we note that for low and intermediate $\tan\beta$, the RGE can be solved for the right selectron, \tilde{e}_R , and $\tilde{\chi}_1^0$ masses to give at the electroweak scale:

$$\begin{aligned} m_{\tilde{e}_R} &= m_0^2 + 0.15m_{1/2}^2 - \sin^2\theta_W M_W^2 \cos 2\beta \\ m_{\tilde{\chi}_1^0} &= 0.16m_{1/2}^2 \end{aligned} \tag{4}$$

where the numerical factors come from solving the RGE. The last term is about $(35\text{GeV})^2$, and so for $m_0 = 0$, the \tilde{e}_R becomes degenerate with the $\tilde{\chi}_1^0$ at $m_{1/2} \simeq 350$ GeV, and thus co-annihilation begins at $m_{1/2} \simeq (350 - 400)\text{GeV}$. As $m_{1/2}$ increases, m_0 must be raised in lock step (to keep $m_{\tilde{e}_R} > m_{\tilde{\chi}_1^0}$). More, precisely, it is the light stau, which is the lightest slepton, that dominates the co-annihilation phenomena. However, one ends up

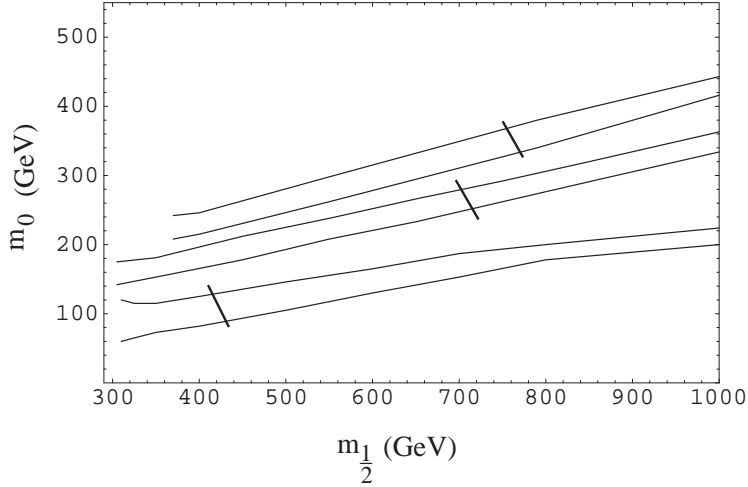


Figure 1: Corridors in the $m_0 - m_{1/2}$ plane allowed by the relic density constraints for (bottom to top) $\tan \beta = 10, 30, 40, A_0 = 0$ and $\mu > 0$. The lower bound on $m_{1/2}$ is due to the m_h lower bound for $\tan \beta = 10$, due to the $b \rightarrow s\gamma$ bound for $\tan \beta = 40$, while both these contribute equally for $\tan \beta = 30$. The short lines cutting the channels represent upper bound from the $g_\mu - 2$ experiment. [24]

with corridors in the $m_0 - m_{1/2}$ plane with allowed relic density, with m_0 closely correlated with $m_{1/2}$ and m_0 increasing as $m_{1/2}$ increases.

We now turn to the other experimental constraints. The Higgs mass bound and the $b \rightarrow s\gamma$ bounds produce comparable constraints on the parameter space, the Higgs mass generally being dominant for low $\tan \beta$ and the $b \rightarrow s\gamma$ for high $\tan \beta$. Over the entire $\tan \beta$ range these constraints produce a lower bound on $m_{1/2}$:

$$m_{1/2} \geq (300 - 400)\text{GeV} \quad (5)$$

corresponding to a lower bound on the neutralino mass of

$$m_{\tilde{\chi}_1^0} \geq (120 - 160)\text{GeV} \quad (6)$$

This means that most of the parameter space is in the $\tilde{\tau} - \tilde{\chi}_1^0$ co-annihilation domain in the relic density calculation. Thus relic density bounds then imply m_0 is approximately determined by $m_{1/2}$.

If we now include the Brookhaven $g_\mu - 2$ constraint we obtain additional restrictions on the parameter space. First the sign of a_μ^{SUGRA} implies that $\mu > 0$. Further, the lower bound on a_μ^{SUGRA} implies an upper bound on $m_{1/2}$. Thus for $A_0 = 0$, one has $m_{1/2} < 440$ GeV for $\tan \beta = 10$, $m_{1/2} < 790$ for $\tan \beta = 40$ and $m_{1/2} < 850$ for $\tan \beta = 50$. Thus assuming the Brookhaven E821 data, we obtain both an upper bound on $m_{1/2}$ and a lower bound on $m_{1/2}$. The reduction of the parameter space for small $\tan \beta$ then puts a lower

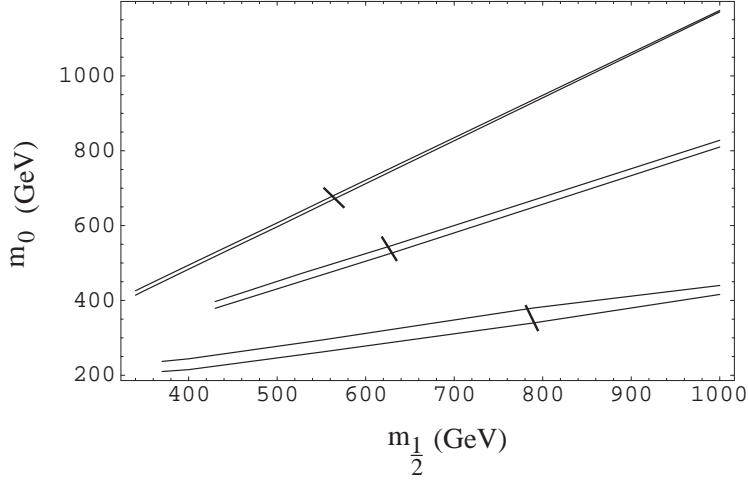


Figure 2: Corridors in the $m_0 - m_{1/2}$ plane allowed by the relic density constraint for $\tan\beta = 40$, $\mu > 0$ and (bottom to top) $A_0 = 0, -2m_{1/2}, 4m_{1/2}$. the curves terminate at the lower end due to the $b \rightarrow s\gamma$ constraint except for $A_0 = 4m_{1/2}$ which terminates due to the m_h constraint. The short lines cutting the corridors represent the upper bound on $m_{1/2}$ due to the $g_\mu - 2$ experiment. [25]

bound on $\tan\beta$. We find

$$\tan\beta > 7(5), \text{ for } A_0 = 0(-4m_{1/2}) \quad (7)$$

Some of the above results are illustrated in Figs. 1 and 2. Fig. 1 shows the allowed regions (which are the co-annihilation channels) in the $m_0 - m_{1/2}$ plane for $\tan\beta = 10, 30, 40$ (from bottom to top) for $A_0 = 0$ [24]. The lower $m_{1/2}$ bounds are due to the m_h bound for $\tan\beta = 10$, and due to the $b \rightarrow s\gamma$ bound for $\tan\beta = 40$. (They are equally constraining for $\tan\beta = 30$.) The $g_\mu - 2$ upper bounds are given by the short lines cutting the channels. One sees that the co-annihilation corridors occur for higher m_0 as $\tan\beta$ increases. Fig. 2 shows the A_0 dependence for the case of $\tan\beta = 40$. One sees that the co-annihilation corridors lie higher in m_0 for A_0 different from zero.

For $\tan\beta > 50$, a new phenomena arises due to the fact that the heavy Higgs (H, A) become light, and can contribute to the annihilation cross section. Results in this domain become very sensitive to the precise values of m_t and m_b [26]. We illustrate this in Figs. 3 and 4. Fig. 3 gives the allowed region in the $m_0 - m_{1/2}$ plane for $\tan\beta = 50$, $A_0 = 0$ using the central experimental values of $m_t = 175$ GeV and $m_b = 4.25$. However, if m_t is reduced by 1σ to 170 GeV, one sees from Fig. 4, that the shape of the allowed region is significantly modified, and a new corridor is opened at low $m_{1/2}$ rising to $m_0 > 1$ TeV.

We see that the parameter space has become highly restricted, both at the lower end and the upper end, and this should help in clarifying the predictions for dark matter detection. The general features of $\sigma_{\tilde{\chi}_1^0 - p}$ that explain its properties are that $\sigma_{\tilde{\chi}_1^0 - p}$ increases

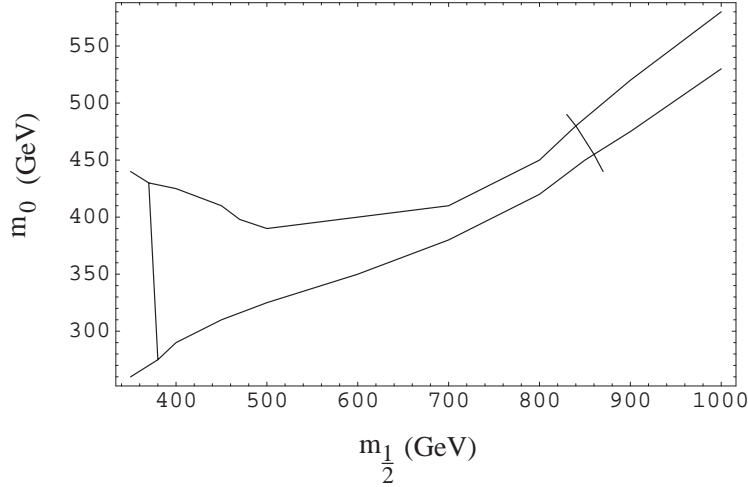


Figure 3: Allowed region in the $m_0 - m_{1/2}$ plane for $\tan\beta = 50$, $A_0 = 0$, $\mu > 0$ for $m_t = 175$ GeV, $m_b = 4.25$. The lower and upper bounds on $m_{1/2}$ are due to the $b \rightarrow s\gamma$ and a_μ constraints respectively.

with increasing $\tan\beta$, and decreases with increasing $m_{1/2}$ and m_0 (and as we've seen, $m_{1/2}$ and m_0 move together). Thus the maximum values of $\sigma_{\tilde{\chi}_1^0-p}$ are generally expected to occur for high $\tan\beta$, and low $m_{1/2}$, m_0 . We now return to our two questions of Sec. 1: in mSUGRA, how large can cross sections get, i. e. can they accommodate the DAMA data, and how small can they become, i. e. will future detectors be able to scan the entire parameter space. The current DAMA annual modulation signal is in the range [27]

$$(\sigma_{\text{wimp}})_{\text{DAMA}} \simeq (10^{-5} - 10^{-6})\text{pb and } m_{\text{wimp}} \leq (100 - 300)\text{GeV} \quad (8)$$

where the uncertainty in the upper bound on the wimp mass being due in part to astronomical uncertainties about the Milky Way. We compare this now to the mSUGRA predictions. Fig. 5 shows the A_0 dependence of the cross sections for $\tan\beta = 40$. Note that $A_0 = 0$ gives the largest cross section. We see that it is the low $m_{1/2}$ bound that prevents the cross section from becoming large, (and in fact if the bound on m_h were to increase to 120 GeV, the lower bound on $m_{1/2}$ would rise to 200 GeV for $A_0 = -2m_{1/2}$, to 215 GeV for $A_0 = 0$, and to 246 GeV for $A_0 = 4m_{1/2}$ further reducing the maximum cross sections). Fig. 6 shows the cross sections for $\tan\beta = 10, 30, 40$ and 50 for $A_0 = 0$, $m_t = 175$ GeV. The largest cross sections occur for the largest $\tan\beta$ and smallest $m_{1/2}$, as expected. We find in general,

$$\sigma_{\tilde{\chi}_1^0-p} < (0.07) \times 10^{-6}\text{pb for } \tan\beta < 50 \quad (9)$$

which is well below the DAMA bound. Thus it is not possible for the mSUGRA model to accommodate the DAMA data. We note that central in this result is the m_h and $b \rightarrow s\gamma$ constraints which put a lower bound on $m_{1/2}$ and hence require $m_{\tilde{\chi}_1^0}$ to be relatively high.

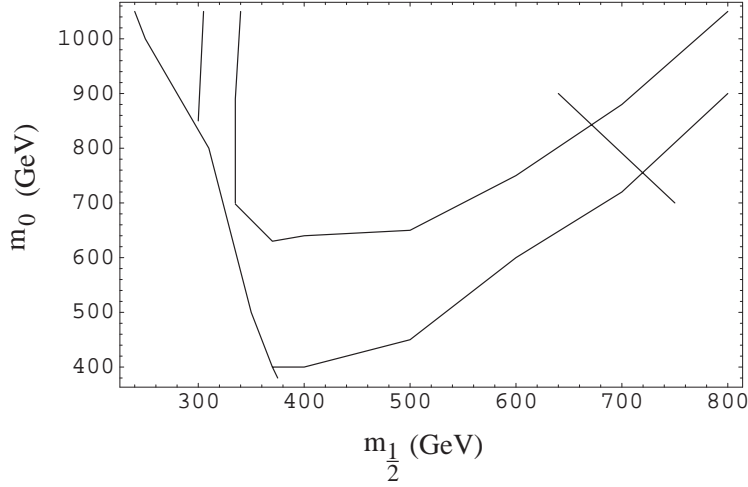


Figure 4: Allowed regions in the $m_0 - m_{1/2}$ plane for $\tan\beta = 50$, $A_0 = 0$, $\mu > 0$ for $m_t = 170$ GeV, $m_b = 4.25$ GeV. The lower and upper bounds on $m_{1/2}$ are due to the $b \rightarrow s\gamma$ and a_μ constraints respectively.

We turn now to the second question, what are the minimum values possible for $\sigma_{\tilde{\chi}_1^0-p}$, and will future detectors being planned be able to observe them. Minimum cross sections arise from low $\tan\beta$ and large $m_{1/2}$, m_0 . Here the question of the validity of the Brookhaven $g_\mu - 2$ data plays an important role in two ways. First this data would eliminate the $\mu < 0$ possibility and for $\mu < 0$, there are accidental cancellations that can reduce $\sigma_{\tilde{\chi}_1^0-p}$ to well below 10^{-10} pb over wide ranges of parameters [18, 28], which would make this part of the parameter space experimentally inaccessible. Thus these extremely low cross sections would be eliminated. Second, it is the lower bound on a_μ^{SUGRA} that produces the upper bound on $m_{1/2}$, and this effect is larger for smaller $\tan\beta$ (see e. g. Fig. 6) moderating the reduction of the cross section as $\tan\beta$ decreases. Fig. 7 shows $\sigma_{\tilde{\chi}_1^0-p}$ for $\tan\beta = 10$, $A_0 = 0$ (upper curve), $-4m_{1/2}$ (lower curve). We see here that $\sigma_{\tilde{\chi}_1^0-p} > 4 \times 10^{-10}$ pb. The parameter space ends for $\tan\beta = 7$ (5) for $A_0 = 0$ ($-4m_{1/2}$) and in general one finds $\sigma_{\tilde{\chi}_1^0-p} \geq 10^{-10}$ pb.

Future detectors hope to obtain a sensitivity of $\sigma_{\tilde{\chi}_1^0-p} \simeq (10^{-9} - 10^{-10})$ pb. Thus they should be able to scan most of the mSUGRA parameter space. If this sensitivity is achievable, dark matter experiments would be competitive with accelerator experiments.

4 Non-Universal Models

We next investigate the possibility that the DAMA data gets confirmed, and the large neutralino -proton cross sections it implies are correct. To accommodate this theoretically, one can consider models with non-universal soft breaking at M_G in the Higgs and third

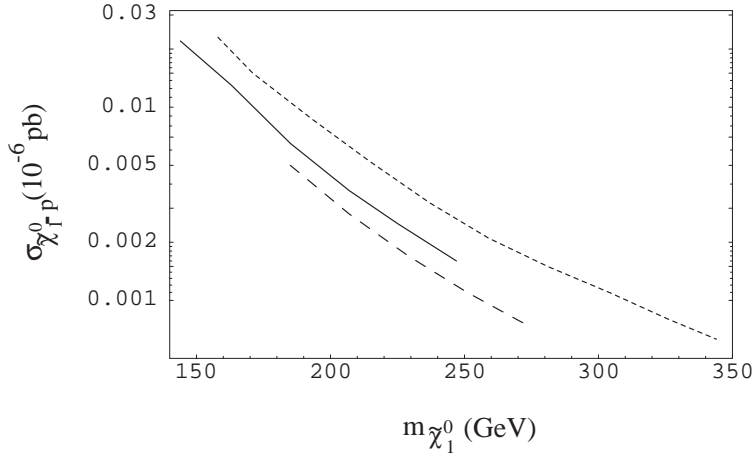


Figure 5: $\sigma_{\tilde{\chi}_1^0-p}$ for $\tan\beta = 40$, $\mu > 0$, for (bottom to top), $A_0 = -2m_{1/2}$, $A_0 = 4m_{1/2}$, $A_0 = 0$. The lower bounds on $m_{\tilde{\chi}_1^0}$ are as in Fig. 2.

generation squarks and sleptons. A convenient parameterization is

$$\begin{aligned}
m_{H_1}^2 &= m_0^2(1 + \delta_1); & m_{H_2}^2 &= m_0^2(1 + \delta_2); \\
m_{q_L}^2 &= m_0^2(1 + \delta_3); & m_{t_R}^2 &= m_0^2(1 + \delta_4); & m_{\tau_R}^2 &= m_0^2(1 + \delta_5); \\
m_{b_R}^2 &= m_0^2(1 + \delta_6); & m_{l_L}^2 &= m_0^2(1 + \delta_7).
\end{aligned} \tag{10}$$

with $-1 \leq \delta_i \leq 1$. While this appears to involve introducing a large number of new parameters, one can understand the effects they produce relatively simply, as much of the physics of what occurs is governed by the μ parameter. One can qualitatively see the effects of the non-universalities for low and intermediate $\tan\beta$ where one may solve the RGE for μ^2 analytically [29]:

$$\begin{aligned}
\mu^2 &= \frac{t^2}{t^2 - 1} \left[\left(\frac{1 - 3D_0}{2} + \frac{1}{t^2} \right) + \frac{1 - D_0}{2} (\delta_3 + \delta_4) \right. \\
&\quad \left. - \frac{1 + D_0}{2} \delta_2 + \frac{\delta_1}{t^2} \right] m_0^2 + \text{universal parts} + \text{loop corrections}.
\end{aligned} \tag{11}$$

where $t = \tan\beta$ and $D_0 = 1 - (m_t/200 \sin 2\beta)^2$. One sees that D_0 is small (i. e. $D_0 \cong 0.25$) and that the universal contribution to the m_0^2 term nearly cancels out. Thus one does not need a large amount of non-universality for the δ_i contributions to dominate. Now the important point is that if μ^2 decreases (increasing the Higgsino content of $\tilde{\chi}_1^0$) $\sigma_{\tilde{\chi}_1^0-p}$ increases, and similarly if μ^2 increases, $\sigma_{\tilde{\chi}_1^0-p}$ decreases (though by not as large an amount). From Eq(11), then we see that the cross section increases if $\delta_{1,3,4} < 0, \delta_2 > 0$. We consider here a simple $SU(5)$ model where $\delta_{10} \equiv \delta_3 = \delta_4 = \delta_5$, and $\delta_{\bar{5}} \equiv \delta_6 = \delta_7$. We chose $\delta_1 = -1, \delta_2 = 1$, with $\delta_{\bar{5}} > 0$ and $\delta_{10} < 0$. With these choices, μ^2 is reduced and hence

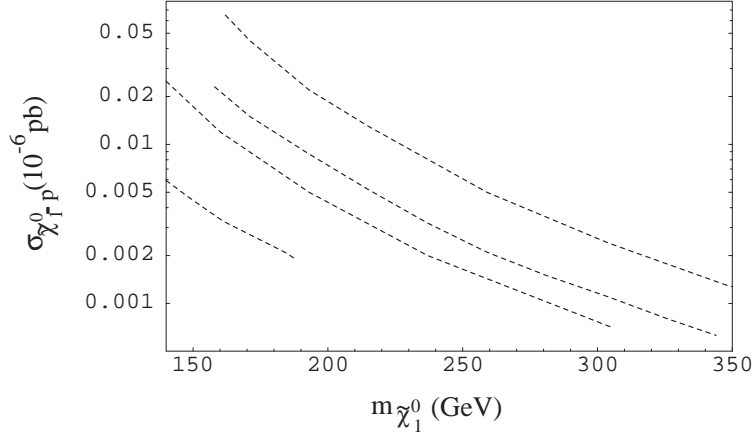


Figure 6: $\sigma_{\tilde{\chi}_1^0-p}$ for $A_0 = 0$, $m_t = 175$ GeV, $m_b = 4.25$, for $\tan \beta = 10, 30, 40, 50$ (from bottom to top). The lower bound on $m_{\tilde{\chi}_1^0}$ is due to the $b \rightarrow s\gamma$ constraint for $\tan \beta = 30, 40, 50$, and from the m_h constraint for $\tan \beta = 10$.

the cross section is increased. One must, however, make sure the relic density constraint is simultaneously satisfied. This occurs due to the fact that the δ_i chosen also lowers m_A . Thus the RGE for m_A give for low and intermediate $\tan \beta$:

$$m_A^2 = \frac{t^2 + 1}{t^2 - 1} \left[\frac{3(1 - D_0)}{2} + \frac{1 - D_0}{2} (\delta_3 + \delta_4) - \frac{1 + D_0}{2} \delta_2 + \delta_1 \right] m_0^2 + \text{universal parts} + \text{loop corrections}. \quad (12)$$

Thus m_A is simultaneously lowered opening an annihilation channel for $\tilde{\chi}_1^0$ through an A s-channel pole, and allowing the relic density constraint to be satisfied. What is happening is similar to what happens in mSUGRA at $\tan \beta \geq 50$, but for the non-universal model this effect can happen at low $\tan \beta$ and with a significantly larger effect. Fig. 8 shows the maximum value of $\sigma_{\tilde{\chi}_1^0-p}$ for the model discussed above for $\tan \beta = 12$ (lower curve), 18 (upper curve). One sees that one can generate $\sigma_{\tilde{\chi}_1^0-p}$ in the DAMA domain for $\tan \beta \gtrsim 15$. Note also that the lower bound on $m_{\tilde{\chi}_1^0}$ is greatly reduced, since the Higgs mass and $b \rightarrow s\gamma$ constraints are much less confining for the non-universal model. (Again a lower wimp mass would be in better accord with the DAMA results.) Thus if the DAMA data is confirmed by other groups, this could point to the validity of non-universal SUGRA models.

The minimal cross sections arise from low $\tan \beta$, large $m_{1/2}$, m_0 and also from reversing the signs of the δ_i . One finds for $\mu > 0$ (as implied by the $g_\mu - 2$ data) that $\sigma_{\tilde{\chi}_1^0-p} \geq 10^{-10} \text{pb}$, which as before is within the reach of future planned detectors.

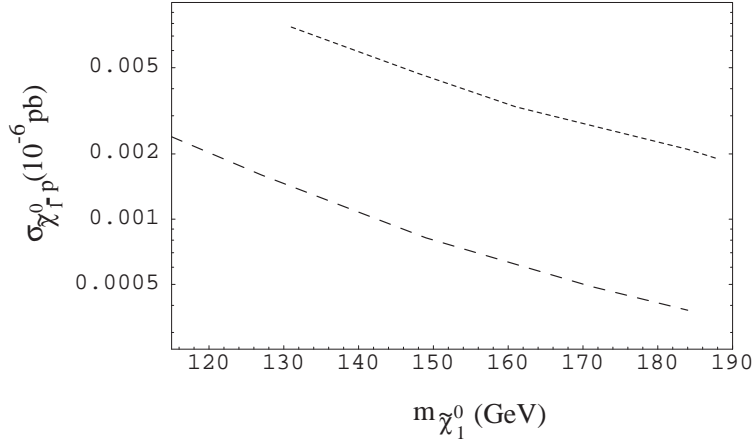


Figure 7: $\sigma_{\tilde{\chi}_1^0-p}$ for $\tan\beta = 10$, $A_0 = 0$ (upper curve), $A_0 = -4m_{1/2}$ (lower curve). The lower bound on $m_{\tilde{\chi}_1^0}$ is due to the m_h bound for $A_0 = 0$, and the $b \rightarrow s\gamma$ constraint for $A_0 = -4m_{1/2}$.

5 Conclusions

We have discussed here the direct detection of neutralino dark matter in the Milky Way within the framework of R-parity conserving gravity mediated supergravity models with grand unification at $M_G \cong 2 \times 10^{16}$ GeV. In particular, we examined two questions: if the DAMA data is confirmed, can SUGRA models accommodate the large cross sections implied by the data, and also, what are the lowest cross section the SUGRA theory predicts and will future planned detectors be able to scan the entire parameter space.

There are now many experimental constraints that allow one to make clearer predictions for these models. Thus for mSUGRA, the Higgs mass and $b \rightarrow s\gamma$ constraints create a lower bound of $m_{1/2} \geq (300 - 400)$ GeV (i.e. $m_{\tilde{\chi}_1^0} \geq (120 - 160)$ GeV), which puts the parameter space mainly in the co-annihilation domain, and (approximately) determines m_0 in terms of $m_{1/2}$ (for fixed $\tan\beta$ and A_0). We find then that the largest cross section is significantly below the lower bound of the DAMA data for $\tan\beta < 50$. (For $\tan\beta \geq 50$, predictions are sensitive to the precise values of m_t and m_b .) If the muon $g - 2$ anomaly is confirmed by future data, then significant further reduction of the parameter space occurs. One has that μ is positive, eliminating the possibility of very small cross sections. In addition, this effect produces an upper bound of $m_{1/2} < 850$ GeV for $\tan\beta < 50$ as well as a lower bound on $\tan\beta$ of $\tan\beta > 7$ (5) for $A_0 = 0$ ($-4m_{1/2}$). We find then over the remaining parameter space that cross sections are greater than $\simeq 10^{-10}$ pb and hence most of the parameter space will be accessible to the future planned experiments. This result also holds without the $g_\mu - 2$ anomaly for the $\mu > 0$, $m_{1/2} \leq 1$ TeV part of the parameter space.

For non-minimal SUGRA models, with non-universal soft breaking in the Higgs and

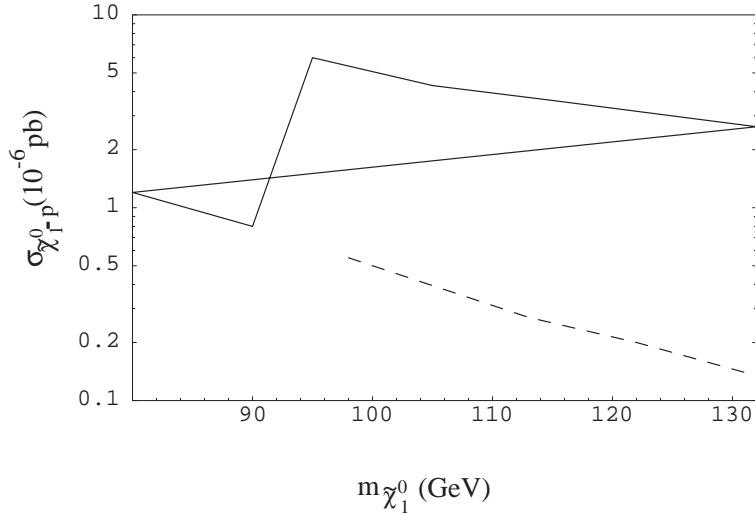


Figure 8: Maximum values of $\sigma_{\tilde{\chi}_1^0-p}$ for $\tan\beta = 12$ (lower curve), 18 (upper curve) for $\delta_2 = 1 = -\delta_1$, $\delta_{10} < 0$, $\delta_5 > 0$, $A_0 = 0$, $\mu > 0$.

third generation squark and slepton sectors, one can generate models with significantly larger neutralino-proton cross sections. Thus for a simple SU(5) model, one finds it is possible to find cross sections in the DAMA region for $\tan\beta > 15$, and also the lower bound on the neutralino mass can be reduced to 80 GeV. These models satisfy the relic density constraint by simultaneously reducing the A mass (even for the relatively low $\tan\beta$ above), and one also finds that for the $\mu > 0$ part of the parameter space the cross sections should not fall significantly below 10^{-10} pb, and thus be experimentally accessible.

ACKNOWLEDGEMENTS

This work was supported in part by National Science Foundation Grant PHY-0101015.

References

- [1] A.H. Chamseddine, R. Arnowitt, P. Nath, Phys. Rev. Lett. **49** (1982) 970.
- [2] R. Barbieri, S. Ferrara, C.A. Savoy, Phys. Lett. B**119** (1982) 343; L. Hall, J. Lykken, S. Weinberg, Phys. Rev. D**27** (1983) (2359); P. Nath, R. Arnowitt, A.H. Chamseddine, Nucl. Phys. B**227** (1983) (121).
- [3] G.L. Kane, L.-T. Wang, J.D. Wells, hep-ph/0108138.

- [4] E.A. Baltz, J. Edsjo, K. Freese, P. Gondolo, astro-ph/0109318.
- [5] V. Barger, F. Halzen, D. Hooper, C. Kao, hep-ph/0105182.
- [6] A. Bottino, N. Fornengo, S. Scopel, F. Donato, hep-ph/0105233.
- [7] P. Igo-Kemenes, LEPC meeting, November 3, 2000 (<http://lephiggs.web.cern.ch/LEPHIGGS/talks/index.html>).
- [8] M. Alam et al Phys. Rev. Lett. **74** (1995) (2885).
- [9] M. Turner, hep-ph/0106035.
- [10] H.N. Brown et.al., Muon (g-2) Collaboration, Phys. Rev. Lett. **86**, (2001) 2227.
- [11] T.C. Yuan, R. Arnowitt, A.H. Chamseddine, P. Nath, Z. Phys. C **26** (1984) 407.
- [12] D.A. Kosower, L.M. Krauss, N. Sakai, Phys. Lett. B **133** (1983) 305.
- [13] K. Melnikov, Int. J. Mod. Phys. A **16** (2001) 4591.
- [14] R. Rattazi, U. Sarid, Phys. Rev. D **53** (1996) (1553).
- [15] M. Carena, M. Olechowski, S. Pokorski, C. Wagner Nucl. Phys. B **426** (1994) (269).
- [16] G. Degrandi, P. Gambino, G. Giudice, JHEP **0012** (2000) 009.
- [17] M. Carena, D. Garcia, U. Nierste, C. Wagner, Phys. Lett. B **499** (2001) 141.
- [18] R. Arnowitt, B. Dutta, Y. Santos, hep-ph/0010244; hep-ph/0101020; Nucl. Phys. B **606** (2001) 59.
- [19] J. Ellis, T. Falk, G. Gani, K. Olive, M. Srednicki, Phys. Lett. B **570** (2001) 236; J. Ellis, T. Falk, K. Olive, Phys. Lett. B **444** (367) 1998; J. Ellis, T. Falk, K. Olive, M. Srednicki, Astropart. Phys. **13** (2000) 181; Erratum-ibid. **15**, (2001) 413.
- [20] M. Gomez, J. Vergados, hep-ph/0012020; M. Gomez, G. Lazarides, C. Pallis, Phys. Rev. D **61** (2000) 123512; Phys. Lett. **B487**, (2000) 313; L. Roszkowski, R. Austri, T. Nihei, JHEP **0108**, (2001) 024; A. Lahanas, D. Nanopoulos, V. Spanos, Phys. Lett. B **518** (2001) 94 and talk by V. Spanos at this conference.
- [21] See e.g., M.B. Green, J.H. Schwarz, E. Witten, "Superstring theory", vol.2, Sec.16.4 (Cambridge University Press, Cambridge, 1987).
- [22] M. Olsson, Phys. Lett. B **482** (2000) 50.
- [23] M. Pavan, R. Arndt, I. Strakovsky, R. Workman, PiN Newslett. **15** (1999) 118.

- [24] R. Arnowitt, B. Dutta, Y. Santoso, Phys. Rev. D **64** (2001) 113010.
- [25] R. Arnowitt, B. Dutta, B. Hu, Y. Santoso, Phys. Lett. **B505**, (2001) 177.
- [26] J. Ellis, T. Falk, G. Ganis, T. Vergata, K. Olive, M. Srednicki, Phys. Lett. **B510**, (2001) 236; J. Ellis, S. Heinemeyer, K. Olive, G. Weiglein, Phys. Lett. **B515**, (2001), 348.
- [27] P. Belli et.al. hep-ph/0112018, talk at this conference.
- [28] J. Ellis, A. Ferstl, K. A. Olive, Phys. Lett. B **481** (2001) 304; Phys. Rev. D **63** (2001) 065016.
- [29] R. Arnowitt, P. Nath, Phys. Rev. D **56** (1997) 2820.